Desalination and Water Treatment
www.deswater.com
doi: 10.1080/19443994.2012.760111

51 (2013) 5710–5720
August

Taylor & Francis
Taylor & Francis Group

Removal of ammonium from water by adsorption onto synthetic zeolites NaA and NaX: a comparative parametric, kinetic, and equilibrium study

Gholamreza Moussavi[a,*], Sadegh Talebi[a], Mehrdad Farohki[b], Robabeh Mojtabaee Sabouti[c]

[a]*Department of Environmental Health Engineering, Tarbiat Modares University, Tehran, Iran*
Tel. +98 21 82883827; Fax: +98 21 82883825; email: moussavi@modares.ac.ir
[b]*Department of Environmental Health Engineering, Guilan University of Medical Sciences, Rasht, Iran*
[c]*Guilan Rural Water and Wastewater Co., Rasht, Iran*

Received 7 October 2012; Accepted 14 December 2012

ABSTRACT

The capability of two synthetic zeolites, NaA and NaX, to remove ammonia nitrogen from water was examined. NaA and NaX were porous zeolites with an average particle diameter of 316 and 460 nm, average pore diameter of 0.4 and 0.8 nm, and BET of 177 and 271 m^2/g, respectively. The influence of various experimental conditions on ammonium removal by NaA and NaX zeolites was investigated. The optimum pH for ammonium removal using NaA and NaX was found to be 7, at which 70.2% and, approximately, 80% of 50 mg N/L ammonium was removed, respectively, at an optimum zeolite concentration of 4 g/L of Na. The ammonium removal data for both zeolites were best fitted with a pseudo-second-order adsorption reaction model. The adsorption of ammonium on the zeolite particles could be better described by the Freundlich model. The maximum adsorption capacity of NaA and NaX was 94.2 and 161.3 mg N/g, respectively, under optimum water pH. These findings reveal that the NaX synthetic zeolite can be an efficient material for adsorbing ammonium from polluted waters.

Keywords: Synthetic zeolite; NaA; NaX; Adsorption; Ammonium

1. Introduction

Zeolites are hydrated aluminosilicate porous materials with a tetrahedron framework [1]. Zeolites are found naturally in different geological formations throughout the world. Due to their abundance in nature as well as their unique futures, including ion-exchanging, molecular sieving, catalyzing, and sorbing capabilities [1], these materials have garnered much worldwide attention with respect to the elimination of various organic and inorganic contaminants from water, wastewater, and waste air streams. Wang et al. [1] has recently reviewed the literature published on the application of zeolite for the removal of contaminants from water and wastewater streams. From their report, it is clearly found that zeolites have considerable potential for the elimination of different classes of environmental contaminants. Nevertheless, the main challenge in the application of natural zeolites is their low specific surface area and heterogeneity of

---

*Corresponding author.

pores leading to their relatively low rate and capacity in adsorption contaminants. This requires designing a large adsorption vessel and frequent bed replacement/remediation making the treatment process complex and costly. These defects have focused studies on the preparation of synthetic zeolites with homogenous pores and higher specific surface area than those of natural zeolites [2]. Due to these features, synthetic zeolites have found many industrial applications, particularly as adsorbents/ion exchange, molecular sieves, and catalysts [3]. The adsorption/ion exchanging potential of synthetic zeolites has led to their synthesis and application for the removal of various contaminants from waste streams. The literature indicates that so far, various zeolites have been synthesized and used for the removal of different contaminants including Zn^{2+} and Cu^{2+} onto NaX [3], ethyl mercaptan onto NaX [4], ammonium onto NaX [5] and NaA [2], Zn^{2+} onto NaA and NaX [6], UO_2^{2+} onto NaA [7], and ammonium onto zeolites synthesized from low-calcium and high-calcium fly ashes [8].

In the present study, ammonium was selected as the target contaminant to investigate its removal from water using two nano-sized synthetic zeolites: NaA and NaX. The presence of ammonia nitrogen is an indication of contamination of a water source with wastewater [5,9]. To prevent its detrimental effects, ammonia nitrogen must be eliminated from the contaminated water before being used for drinking or for some specific industrial purposes. As stated above, Zheng et al. [5] evaluated the adsorption characteristic of a zeolite, 13X, with a particle size of 4–6 mm in the removal of ammonium from aqueous solution. Also, Zhao et al. [2] investigated the potential of a micron-sized NaA zeolite prepared from halloysite mineral for the adsorption of ammonium ions and observed a maximum adsorption capacity of 44.3 mg/g of ammonium. However, because the composition and structure of synthetic zeolites have a great influence on their removal efficacy with respect to a given contaminant, further research regarding the synthesis and application of new zeolites is still required to confirm their potential in the removal of the desired contaminant.

Accordingly, the present study was conducted to examine and compare the capability of two synthetic zeolites (NaA and NaX) for removing ammonia nitrogen from an aqueous solution. The influences of basic variables, including the pH of the solution, zeolite concentrations, reaction time, and ammonia nitrogen concentration on the removal of ammonia nitrogen were investigated. The isotherm and kinetics of ammonia nitrogen adsorption onto each of the selected zeolite were also evaluated.

2. Materials and methods

2.1. Materials

Powdered zeolites NaA and NaX were selected in this study as adsorbents. The selected zeolite were purchased from SPAG Co., Iran and used as received. An ammonium stock solution (1%) was made by dissolving NH_4Cl (Merck Co.) in distilled water. The working ammonium solutions were prepared by sufficiently diluting the aliquots of stock solution with distilled water. All other chemicals used were of analytical grade.

2.2. Adsorption experiments

The adsorption experiments were carried out as batch tests in 100-mL glass beakers using 50 mL of ammonium solution as the working volume. The influence of initial pH (2–10), concentration of zeolite (1–6 g/L), and contact time (5–120 min) on the adsorption efficacy were evaluated. For each experiment, a given amount of adsorbent (either NaA or NaX) was added to the bakers containing 50 mL ammonium solution at a known initial concentration and pH. All experiments were conducted at room temperature. The pH of the solution was regulated at the required level using 0.1 N HCl or NaOH solutions. The suspension was then mixed using a Jar test instrument (paddle type mixer) at 100 rpm for a specific time. At the end of the test, the suspension was centrifuged at 10X for 10 min to separate the particles; the supernatant was analyzed for residual ammonium. The efficacy of each zeolite in adsorbing ammonium was evaluated based on the ammonium removal percentage calculated from the following equation:

$$\text{Ammonium removal } (\%) = \frac{(C_0 - C_t)}{C_0} \times 100 \quad (1)$$

2.3. Kinetic experiments

Experiments designed to analyze the kinetics of ammonium adsorption onto the selected zeolite were conducted as batch tests in beakers containing 50 mL of ammonium solution, with the pH regulated at the optimum value obtained from previous experiments.

Each beaker received 0.2 g zeolite powder (NaA or NaX) and was mixed using a Jar test mixer for a given time ranging from 5 to 120 min. The residual concentration of ammonium in each beaker at the end of mixing was determined using the same procedure stated in the previous section. The experimental data were then fitted with pseudo-first-order and pseudo-second-order reaction rate models as well as with an intraparticle diffusion model to understand the kinetics of the adsorption.

2.4. Isotherm experiments

To determine the isotherm of ammonium adsorption onto the NaA or NaX zeolite, experiments were carried out using a series of beakers containing 50 mL ammonium solution with various concentrations ranging from 100 to 400 mg/L and an optimum pH. A constant mass of zeolite (0.1 g) was then added to each vessel and then mixed using the Jar test mixer for 8 h at a constant temperature of 25℃ to ensure that equilibrium was obtained. At the end of each test, the contents of each beaker was centrifuged (as stated above), and the residual concentration of ammonium in the supernatant was determined.

The adsorption capacity, $q_e\,(mg/g)$, which is the amount of ammonium adsorbed onto the zeolite, was calculated from the following mass balance equation:

$$\text{Adsorption capacity }(\text{mg NH}_4^+\text{-N/g}) = \frac{(C_0 - C_e)V}{m} \times 100 \qquad (2)$$

The experimental results were then fitted with the several isotherm classical models to analyze the behavior of ammonium adsorption onto NaA and NaX. All adsorption tests were carried out in duplicate and the average results are presented.

2.5. Analysis

The concentration of ammonia nitrogen in the samples was measured using the Neslerization method detailed in the standard methods [10] and reported as mg NH_4^+-N/L. The concentrations of Na^+ and K^+ were determined using a flame photometer instrument. According to the supplier, the zeolites were characterized for chemical structure, X-ray diffraction (XRD), particle size, pore sizes, and specific surface area by Malvern Instrument Ltd., Malvern, UK. Other characteristics including pH at the point of zero charge (pHpzc), surface morphology, and surface properties (FTIR analysis) were determined upon receiving the materials.

The pHpzc was determined by the titration method using a series of batch tests according to the pH drift procedure [9]. The pH and temperature of the solution were determined by a pH meter (Sense Ion 378, Hack) and thermometer, respectively. The surface morphology of the zeolites was evaluated using scanning electron microscopy (SEM) (Philips-XL30 Electron Microscope). The surface functional groups of the selected zeolites were characterized by FTIR analysis using a Nicolet spectrometer.

3. Results and discussion

3.1. Zeolite characterization

As stated above, the XRD patterns, particle and pore sizes, and specific surface areas of the zeolite were determined by the supplier, and the results were incorporated into this study. According to the supplier information, the XRD patterns of both the zeolites had strong pure peaks at 2θ between 5° and 40°, corresponding to the standard peaks of the crystalline NaA and NaX zeolites. Similar XRD patterns for the synthetic zeolites, NaA and NaX, were also reported by Nibou et al. [6]. The other characteristics of the selected zeolites, NaA and NaX (obtained from the supplier), are given in Table 1. According to the chemical structure of the zeolites shown in Table 1, the Si/Al ratio was 1 and 1.23 in NaA and NaX, respectively. These values are lower than those obtained by Nibou et al. [6], which may be related to the initial template and compounds used as well as to the method of synthesizing the materials. According

Table 1
Chemical structure and main characteristics of zeolite NaX and NaA

Parameter	Unit	Value	
		NaA	NaX
Chemical structure	–	$Na_{12}[(AlO_2)_{12}(SiO_2)_{12}] \cdot 27H_2O$	$Na_{86}[(AlO_2)_{86}(SiO_2)_{106}] \cdot H_2O$
Volume weighted mean particle size	nm	316	460
Average pore diameter	nm	0.4	0.8
Mesopore volume	cm^3/g	0.062	0.165
Micropore volume	cm^3/g	0.176	0.170
BET	m^2/g	177	271
pHpzc	–	~10	~10

to the information given in Table 1, the mean particle sizes of NaA and NaX were 316 and 460 nm and the average sizes of NaA and NaX pores were 0.4 and 0.8 nm, respectively, indicating that both selected materials were nano-sized zeolites. Also, as shown in Table 1, the pores in NaA zeolite were mostly micropores, whereas NaX consisted of similar volume of mesopores and micropores. The BET specific surface areas of NaA and NaX were reported by the supplier to be 177 and 271 m^2/g, respectively. These BET values are lower than those reported in the literature for both NaA and NaX [6]. Indeed, NaX had a greater pore volume and BET value than NaA, and thus a higher adsorption potential is expected for NaX.

The surface morphology of the selected zeolites (NaA and NaX) was observed through the SEM micrographs depicted in Fig. 1. Fig. 1 shows that both NaA and NaX were composed of crystalline particles although the size of the NaA crystals (Fig. 1(a)) was smaller than those of NaX (Fig. 1(b)). Also, the NaA crystals were more clearly faceted than those of NaX, which can be related to a lower concentration of Na in NaA (see Table 1 for chemical formula of zeolites). Nibou et al. [6] observed similar crystal morphology for NaA and NaX synthetic zeolites although they reported different particle sizes, which are attributed to the difference in the zeolites' composition from those used in the present work.

The FTIR spectra of NaA and NaX are illustrated in Fig. 2 (a and b). As shown in Fig. 2(a), the characteristic band in NaA represents hydroxyl group stretching at around 3,441 cm^{-1}, C=O stretching at about 1,655 cm^{-1} [11], and a group of vibration bands ranging from around 1,000 to 470 cm^{-1} representing oxygen bonded with Si and/or Al in a tetrahedral confirmation [6]. Similar peaks were observed for NaX (Fig. 2(b)), although with stronger stretching, which indicates a greater amount of peaks in NaX than NaA. This finding agrees with the chemical formula of the selected zeolite given in Table 1. Another significant observation made from Fig. 2 is that the FTIR spectra of the used zeolite almost overlapped with those of the fresh zeolite revealing that the chemical structure of the zeolite remained unchanged after being used in the treatment process. It can be inferred from this finding that the removed contaminant (ammonium ion) did not engage in chemical interaction with the zeolite surface functional groups.

The pHpzc of both the zeolites was close to 10, indicating that the NaA and NaX had a basic surface, which is related to the presence of hydroxyl groups on the surfaces of both zeolites (Fig. 2). Accordingly, the surface charge of the selected zeolite would be positive at solution with pH below 10 and negative at solution with pH above 10. This characteristic can affect the behavior of contaminant adsorption, which will be explored in the next section.

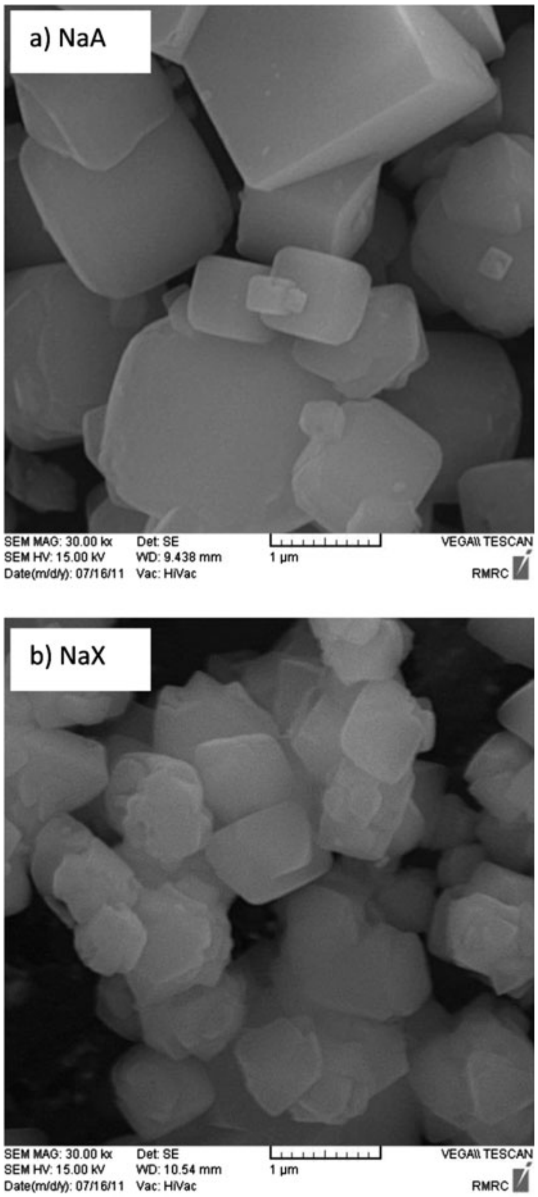

Fig. 1. SEM micrographs of fresh and used (a) NaA and (b) NaX.

3.2. Effect of solution pH

The effect of solution pH between 2 and 10 on the removal of ammonium by NaA and NaX is depicted in Fig. 3. Regarding adsorption onto NaX, Fig. 3 shows that the removal of ammonium increased from 32.4 to 53.8% under the selected conditions when the solution pH was increased from 2 to 7. A further

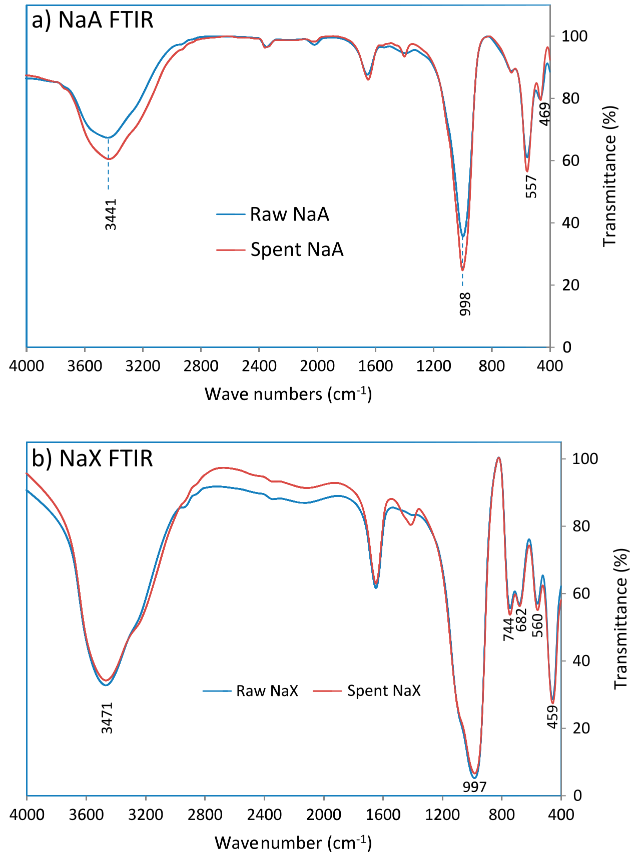

Fig. 2. FTIR spectra of fresh and used (a) NaA and (b) NaX.

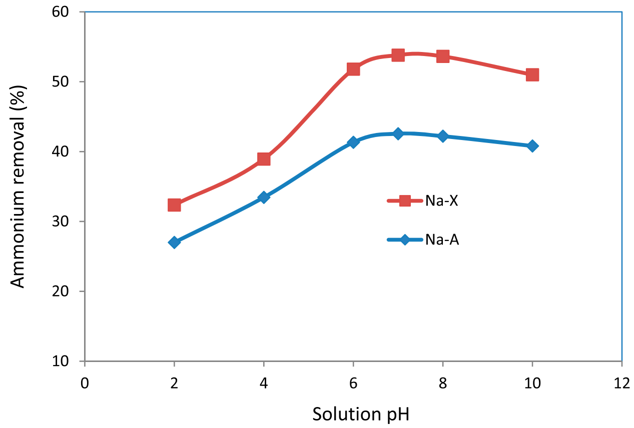

Fig. 3. The effect of solution pH between 2 and 10 on removal of ammonium by zeolite (a) NaA and (b) NaX.

increase in pH from 7 to 10 resulted in the reduction of ammonium removal down to 51.3%. The figure shows that the optimum pH at which the maximum ammonium adsorption could be attained is 7, which lies within the pH range of natural waters. A similar trend was also observed for ammonium adsorption onto NaA, although with a lower percentage at each of the tested pH levels. At the optimum pH, NaX could attain an ammonium removal that was approximately 11% greater than that by NaA indicating the greater efficacy of NaX; the reason for this will be discussed later in the text. This finding is supported by the literature, where the maximum ammonium adsorption by NaA [2] and natural clinoptilolite zeolite [9] was reported to occur at pH 7.

The observed profile of ammonium elimination vs. solution pH by the selected zeolite can be explained by considering the pHpzc of the zeolite, the predominant species of ammonia nitrogen at various pH values, and the surface charge of the zeolite particles at various pH values [9]. According to the zeolite characteristics specified in Section 3.1, the pHpzc of both NaA and NaX was close to 10 suggesting that the surface charge of both the zeolites was positive at solution pH below 10 and negative at solution pH above 10. Also, it is well known that ammonium ions are the predominant species at solution pH below 7, whereas molecular ammonia is the dominant form of ammonium nitrogen beyond natural pH. Accordingly, low ammonium elimination at acidic pH can be related to a competition for available adsorption sites between H^+ and NH_4^+ [9,12]. The higher the solution pH is, the lower the concentration of H^+ would be and thereby, the less H^+ would interfere with ammonium adsorption leading to an increase in ammonium removal. However, reduction in the ammonium removal percentages at solution pH beyond 7 may be due to an increase in the number of ammonia molecules (decrease in the number of ammonium ions) and, thus, a reduction in the degree of interaction between contaminants and active sites on the zeolite surfaces. To understand whether or not the ion-exchange mechanism was involved in the removal of ammonium, the concentration of Na^+ was measured in the solution before and after adsorption. The results reveal (data not shown) no considerable change in Na^+ concentration suggesting that ion exchange was not effective in the ammonium removal achieved by NaA or NaX.

3.3. *Effect of ammonium concentration and contact time*

A critical consideration when applying the adsorption system under given conditions is to provide a sufficient contact time to reduce the contaminant(s) in a contaminated solution with a known concentration to a desired value. Hence, it is technically important to investigate the influence of contact time on the removal of different ammonium concentrations by adsorption onto the selected zeolite. The effect of a contact time between 5 and 120 min was examined on the removal of low (5 g/L) and high (50 mg/L) concentrations of

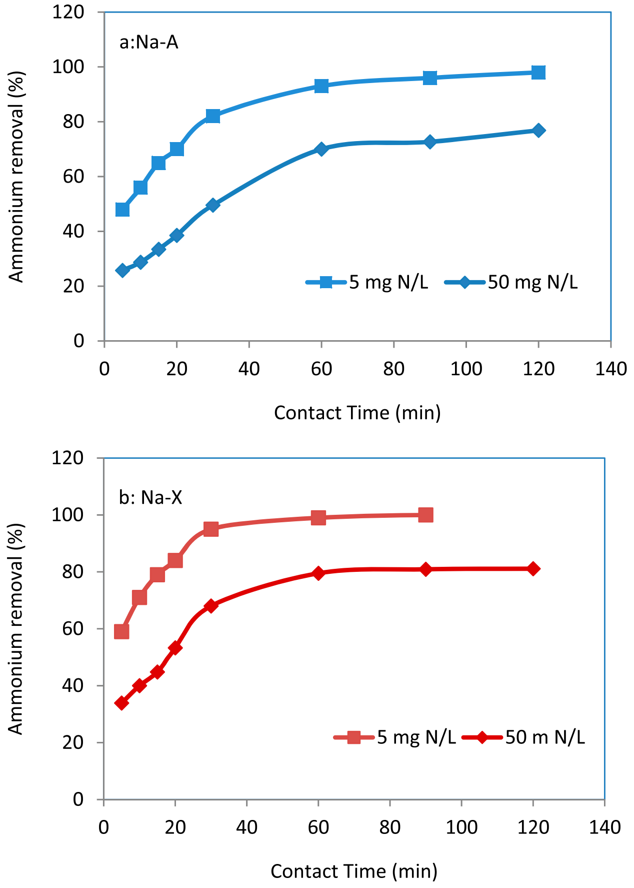

Fig. 4. Ammonium removal efficiency using (a) NaA and (b) NaX as a function of contact time at low (5 mg N/L) and high (50 mg N/L) at optimum pH of 7.

ammonium at the optimum pH value and zeolite concentrations of 7 and 2 g/L, respectively. Fig. 4 presents the results of this phase of study in terms of the removal percentages at low and high concentrations of ammonium by NaA (Fig. 4(a)) and NaX (Fig. 4(b)).

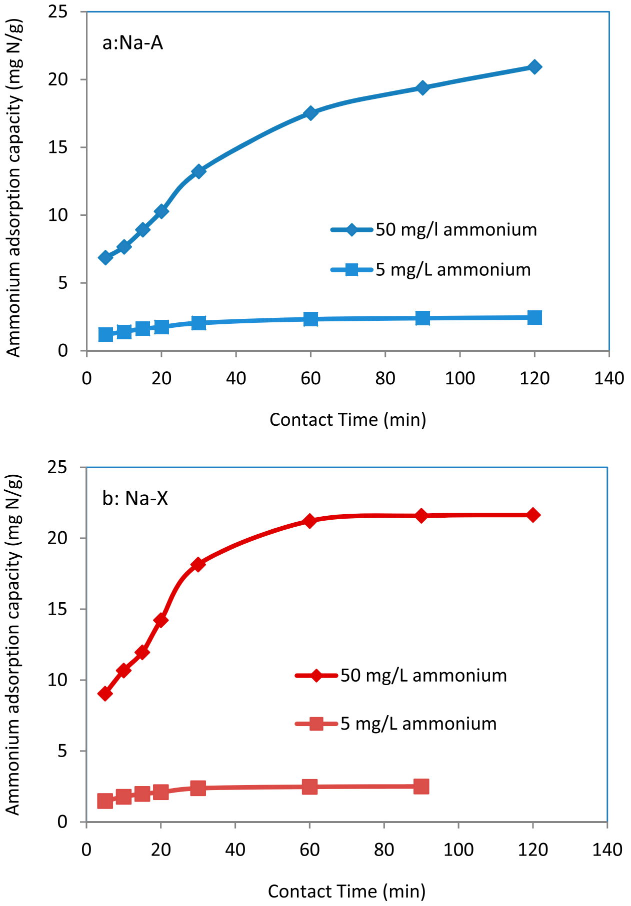

Fig. 5. Ammonium adsorption capacity of (a) NaA and (b) NaX at low (5 mg N/L) and high (50 mg N/L) at the optimum pH of 7.

Based on data shown in Fig. 4(a), the complete removal of ammonium was achieved by zeolite NaX at a low concentration of ammonium and over relatively moderate contact time of 120 min. The removal of ammonium by NaA, however, reached a maximum of 98% over this contact time and under other similar conditions. This reveals the high affinity of NaX for ammonium molecules and, therefore, shows that NaX is an effective adsorbent for the removal of low concentrations of ammonium. The rapid removal of ammonium by NaX can be related to the textural characteristics of the zeolite, which will be discussed later in the text. However, the percentage of ammonium removed over the tested contact times decreased for both zeolites when the ammonium concentration was increased to 50 mg/L (Fig. 4). This decrease reveals the dependency of ammonium removal on the initial concentration, possibly due to a limited number of adsorption/exchange sites and increased intraparticle diffusion. Despite the decrease in the ammonium removal percentages with an increase in concentration, Fig. 5 indicates that the removal capacity increased with the initial ammonium concentration and contact time reaching approximately 20 and 21.3 mg ammonium per g NaA and NaX, respectively, at equilibrium and high ammonium concentration (50 mg/L). This increase (Fig. 4) is attributed to an increase in the number of collisions between ammonium molecules and zeolite with increasing concentration, as well as to the increased concentration gradient and, thus, the mass transfer driving force [13,14] that enhances ammonium molecule uptake by zeolite particles.

3.4. Effect of zeolite concentration

The effect of the concentration of NaA and NaX on ammonium removal was investigated at the optimum

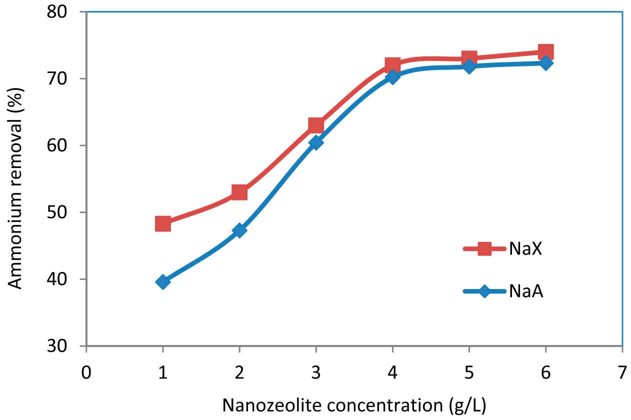

Fig. 6. Ammonium removal efficiency as a function of (a) NaA and (b) NaX concentration (1–6 g/L) at various water temperatures at the optimum pH of 7.

pH of 7, ammonium concentration of 50 mg N/L, and contact time of 60 min. Fig. 6 depicts the average ammonium removal percentages based on triplicate experiments as a function of NaA and NaX concentration. Overall, Fig. 6 shows that the removal of ammonium increased with the increase in the zeolite concentration up to an optimum level for both types of zeolite under the selected experimental conditions.

For zeolite NaA, Fig. 6 shows that the level of ammonium removal increased from 39.6 to 70.2% when the NaA concentration was increased from 1 to 4 g/L; a further increase in adsorbent concentration had no considerable influence on ammonium removal. A similar trend was observed for ammonium removal by zeolite NaX under similar conditions (Fig. 6), although at a higher rate. It is clear from Fig. 6 that when using zeolite NaX as an adsorbent, increasing the adsorbent concentration from 1 to 4 g/L resulted in an improvement in ammonium removal from 53.6 to 79.2% under the selected test conditions; this represents a 25% increase in performance. Similar to that of NaA, the further increase in the NaX concentration to 6 g/L did not significantly affect the ammonium removal percentage. Considering the constant amount of ammonium ions used in all solutions in the experiments, increasing the mass of the adsorbent leads to an increase in the zeolite to ammonium ion ratio, which provides greater surface area and, thus, more sites for exchange/adsorption [15] and a reduction in intraparticle diffusion [16]. This subsequently causes the observed increase in ammonium removal with increasing zeolite concentration up to the optimum level. However, the increase in the adsorbent concentration to a specific level would overcome the limitation in the number of adsorption sites for ammonium ions and, thereby, the removal percentage curve would plateau. Based on these findings, the optimum concentration of each zeolite under the selected conditions was determined to be 2 g/L.

Comparing the plots depicted in Fig. 6 reveals that the ammonium removal percentage was between approximately 9 and 14% greater when using NaX as the adsorbent than when using NaA under similar experimental conditions. In other words, zeolite NaX is more efficient than NaA in removing ammonium from water.

The greater performance of NaX compared to that of NaA can be related to the textural properties of the selected zeolite and the ionic diameter of ammonium. Considering the ionic diameter of ammonium, which is 0.286 nm [17], it is deduced that there was a greater opportunity for the penetration of ammonium ions into the NaX particle pores (0.8 nm) than into the NaA particle pores (0.4 nm), which resulted in greater removal values. Moreover, the specific surface area of NaX is greater than that of NaA (Table 1) thereby, a greater surface per unit of concentration of zeolite is available for adsorption of ammonium molecules in NaX than in NaA. Also, the pore volume of NaX is approximately 40% greater than that of NaA; the micropore volume in both zeolites is almost the same, whereas the mesopore volume is much higher in NaX than in NaA (as given in Table 1). Therefore, the removal of a greater amount of ammonium by NaX, which has a greater mesopore volume than NaA, reveals that ammonium removal by zeolite is likely accomplished by the penetration of ammonium molecules into mesopores.

Because ammonium ions prefer a tetrahedral coordination for strong binding [16], the higher removal percentages of ammonium in NaX than in NaA can be further related to the structure of the zeolite and the fact that NaX is composed of spheres that tetrahedrally bind to oxygen and the Al/Si atoms [3] which were present in greater numbers than in NaA.

3.5. Adsorption kinetics and mechanism

To evaluate the order of the adsorption of RR198 onto the prepared adsorbent, the experimental results from time-course adsorption were fitted with pseudo-first- and pseudo-second-order reaction rate models. The experimental data for ammonium concentrations of 5 and 50 mg/L were fitted to these two models; the kinetics information is summarized in Table 2. Table 2 shows that the pseudo-second-order model had a higher correlation ($R^2 > 0.99$) with the ammonium experimental data for both NaA and NaX. The better fit of the experimental data to the pseudo-second-order model than to the pseudo-first-

Table 2
Summary of kinetic parameters of ammonium adsorption onto NaX and NaA

Zeolite	Initial concentration (mg/L)	1-st order kinetic		2-nd order kinetic		Intraparticle diffusion		
		$[\ln(q_e - q_t) = \ln q_e - k_1 t]$		$[t/q_t = 1/k_2 q_e^2 + t/q_e]$		$[q_t = k_{id} t^{0.5} + C]$		
		k_1	R^2	k_2	R^2	k_{id}	R^2	C
Na-A	5	0.0111	0.7506	0.046	0.9912	0.236		
	50	0.119	0.892	0.002	0.9911	1.665	0.963	3.168
Na-X	5	0.0102	0.6841	0.085	0.9995	0.273		
	50	0.102	0.753	0.004	0.9964	3.996	0.997	−14.6

order rate reveals that both the ammonium and the zeolite concentrations affect the ammonium adsorption process under the investigated conditions [18]. We have also previously reported a pseudo-second-order model for the adsorption of ammonium onto natural zeolite [9]. The lower k_2 value with higher ammonium concentration for both zeolites (Table 1) verifies the improvement in the ammonium mass transfer rate with increased initial ammonium concentration. Table 2 further reveals a higher value k_2 at both low and high ammonium concentrations for ammonium adsorption onto NaX. This confirms the higher affinity of ammonium ions for NaX than for NaA, as was previously ascertained in Section 3.2.

The adsorption of contaminants onto an adsorbent involves four consecutive steps: bulk solution transport, external film resistance to transport (film diffusion), internal pore resistance to transport (intraparticle diffusion), and adsorption; the slowest step limits the adsorption rate [19]. The literature indicates that the first and last steps do not usually limit the adsorption process under experimental conditions [18]. It is, therefore, presumed that either film diffusion or intraparticle diffusion is the rate limiting step. The intraparticle diffusion limitation was checked using the equation developed by Weber and Morris (Table 2) [20]:

The linear relationship between q_t and $t^{0.5}$ when the line is extended from the plot origin indicates that intraparticle diffusion is the only step limiting the adsorption rate [21,22]. The kinetic plot of intraparticle diffusion of ammonium onto either zeolite at two initial concentrations of 5 and 50 mg/L is depicted in Fig. 7. Fig. 7 also clearly shows that the shapes of the plots are different at low and high ammonium concentrations for both zeolite tested.

Referring to Fig. 7, two distinctive regions are observed for the adsorption of a low concentration of ammonium onto both zeolites implying that different adsorption mechanisms are involved at different interval contact times. The first region indicates intraparticle diffusion, the limiting step, and the second indicates that the solution is approaching equilibrium conditions [23,24]. Fig. 7 also shows that for higher ammonium concentrations, the plots obtained from the Weber and Morris equation for both zeolites, NaA and NaX, are one-section plots with a high degree of fitness ($R^2 > 0.99$). This indicates that the intraparticle diffusion is the main step limiting the rate of ammonium adsorption onto NaA and NaX when the contaminant concentration is high. In fact, a high concentration of ammonium in the solution suggests a high concentration gradient and subsequently high diffusion rate of ions from bulk solution to the film

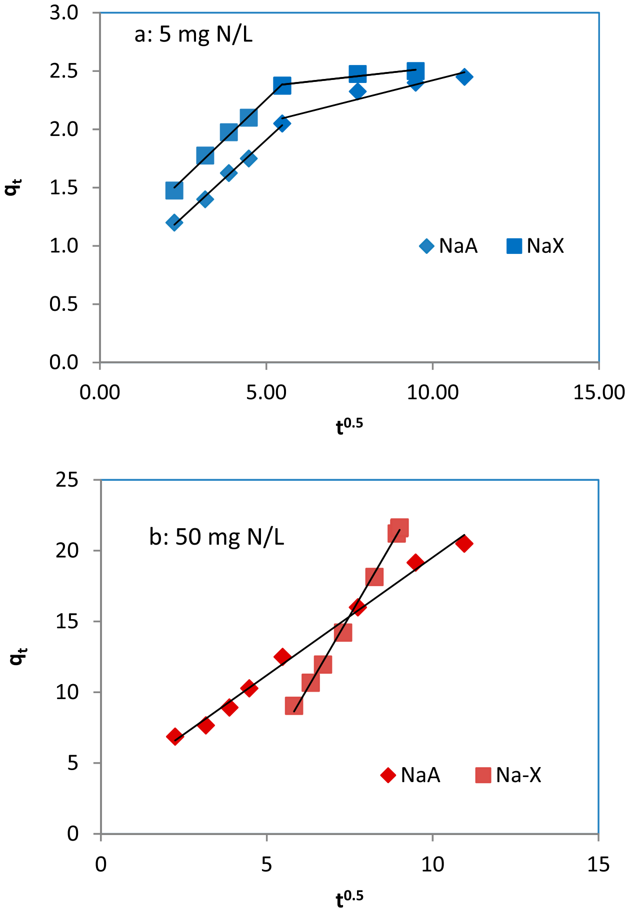

Fig. 7. Plots of intraparticle diffusion equation for adsorption of (a) low and (b) high concentrations of ammonium using NaA and NaX at optimum pH of 7.

layer and thereby to the surfaces of zeolite particles. Therefore, the transport of ammonium molecules into zeolite pores (intraparticle diffusion) is the main step limiting the rate of adsorption and, thus, determining the overall rate of adsorption.

Considering the slope of the regression lines and referring to Table 2, the constants of intraparticle diffusion (k_{id}) for initial ammonium concentrations of 5 and 50 mg/L are found to be 0.236 and 1.665 mg/g. min$^{0.5}$ for zeolite NaA and 0.273 and 3.993 mg/g. min$^{0.5}$ for zeolite NaX, respectively. It is observed that k_{id} assumes a higher value in the adsorption of a higher concentration of ammonium onto both zeolites compared to that in the adsorption of a low ammonium concentration. This confirms the improvement in the adsorption capacity with an increasing initial ammonium concentration. A closer look at Fig. 7 also reveals that for higher ammonium concentrations, the time period during which the intraparticle diffusion is the adsorption rate limiting factor is longer.

3.6. Isotherm modeling

Three of the most commonly applied models—Langmuir, Freundlich, and Dubinin–Radushkevich models—were used to model the adsorption of ammonium onto the NaA and NaX in this study. The linear forms of these equations are shown and the results of the isotherm analysis are given in Table 3. As shown in Table 3, the R^2 of the Freundlich isotherm model is greater than that of the other isotherms for the present adsorption system. The adsorption of ammonium onto the zeolite particles is better described by the Freundlich model, which implies that ammonium adsorption occurs as the adsorption of a multilayer onto a heterogeneous adsorbent surface. No report could be found in the literature on the adsorption of ammonium by zeolite to compare with the obtained data. The best fitness of our experimental data of ammonium adsorption onto NaA and NaX with the Freundlich model in the present work is in accordance with ammonium adsorption onto natural zeolite [9 and references therein] and the synthesized zeolite NaA [2]. However, Zheng et al. [5] reported a Langmuir model as the best fitted isotherm for ammonium adsorption onto NaX. These discrepancies can be related to the structures of the zeolites used as well as the experimental conditions.

Moreover, the experimental data (Table 3) indicate the ammonium adsorption capacities of NaA and NaX as being 59.3 and 89.1 mg N/g, which are considerably higher than those previously reported [2,5]. The higher adsorption capacities of zeolites tested in the present work compared to those reported in the literature can be related to the structural properties and characteristics of the selected zeolites. Indeed, the zeolites used in this study were nano-sized powders with large number of micropores and mesopores, while those reported in the literature were on the order of millimeters [5] and microns [2] in size. Furthermore, the value of the constant n in the Freundlich model, given in Table 3, is greater than unity, which confirms that NaA and NaX are appropriate for use as adsorbents for the removal of ammonium.

According to the D–R isotherm model information given in Table 3, the free energy of ammonium adsorption onto NaA and NaX was 1.08 and 1.32 kJ/mol, respectively. In the D–R isotherm, the value of E indicates the mechanism through which adsorption takes place. A value of E below 8 kJ/mol indicates physical adsorption, and a value between 8 and 16 kJ/mol indicates chemical adsorption [25]. Therefore, the removal of ammonium at the present experiment is likely dominated by physicosorption.

Table 3
Information of isotherm modeling of ammonium adsorption onto NaX and NaA

Model	Unit	Value	
		NaA	NaX
Langmuir [$C_e/q_e = 1/bq_{max} + C_e/q_{max}$]			
R^2		0.859	0.838
b		0.005	0.0048
R_L		0.34–0.67	0.52–0.66
$q_{max\ (model)}$	mg/g	94.2	161.3
$q_{experimental}$	mg/g	59.3	89.1
Freundlich [$\ln q_e = \ln K_F + 1/n \ln C_e$]			
R^2		0.966	0.968
n		1.93	1.69
K_F		3.35	3.1
Dubinin–Radushkevich [$\ln q_e = \ln q_m - K_{DR}\,\varepsilon^2$]			
R^2		0.738	0.747
K_{DR}	mol^2/kJ^2	0.426	0.285
E		1.08	1.32

4. Conclusion

In the present study, two synthetic zeolites, NaA and NaX, were characterized and used for the removal of ammonium from water. The following conclusions were based on the results obtained from the experiment:

(a) NaA and NaX were nano-sized zeolites with particle diameters of 316 and 460 nm, BET of 177 and 271 m^2/g, and average pore diameter of 0.4 and 0.8 nm, respectively.
(b) NaA was mainly a microporous material, while NaX contained both micropores and mesopores.
(c) The maximum ammonium adsorption was obtained at pH 7 and an adsorbent concentration of 4 g/L for both zeolites under the selected conditions.
(d) For both NaA and NaX, the experimental time-course adsorption data most highly correlated with the pseudo-second-order model. The equilibrium adsorption data was best fitted with the Freundlich model.
(e) NaX attained greater ammonia adsorption efficiency than NaA under similar conditions.

Abbreviations

C_0 and C_e — initial and equilibrium ammonium concentrations (mg N/L)
C_t — ammonium concentration at contact time t (mg N/L)
t — adsorption contact time (min)
V — volume of the ammonium solution in the adsorption test flask (mL)
m — mass of zeolite (g)
k_1 — pseudo-first-order adsorption constant (min^{-1})
k_2 — pseudo-second-order adsorption constant ($mg^{-1}\ min^{-1}$)
k_{id} — intraparticle diffusion constant ($mg/g\ min^{0.5}$)
q_t — adsorption capacity at time t (mg N/g)
q_e — adsorption capacity at equilibrium conditions (mg N/g)
C — the plot intercept in Weber and Morris equation
q_{max} — maximum adsorption capacity (mg/g)
b — Langmuir constant (L/mg)
K_F and n — Freundlich constants
$B=RT/b$ — Temkin constant (J/mol)
T — absolute temperature (K)
A — Temkin isotherm constant (L/g)
R — gas constant (8.314 J/mol.K)
K_{DR} — *Dubinin–Radushkevich* constant (mol^2/kJ^2)

$\varepsilon = RT \ln[1 + 1/C_e]$ — Polanyi potential (kJ/mol)

$E = 1/\sqrt{2K_{DR}}$ — adsorption free energy (kJ/mol)

References

[1] S. Wang, Y. Peng, Natural zeolites as effective adsorbents in water and wastewater treatment, Chem. Eng. J. 156 (2010) 11–24.

[2] Y. Zhao, B. Zhang, X. Zhang, J. Wang, J. Liu, R. Chen, Preparation of highly ordered cubic NaA zeolite from halloysite mineral for adsorption of ammonium ions, J. Hazard. Mater. 178 (2010) 658–664.

[3] A. Khelifa, Z. Derriche, A. Bengueddach, Adsorption of propene on NaX zeolite exchanged with Zn^{2+} and Cu^{2+} , Appl. Catal. A 178 (1999) 61–68.

[4] G. Weber, F. Benoit, J.-P. Bellat, C. Paulin, P. Mougin, M. Thomas, Selective adsorption of ethyl mercaptan on NaX zeolite, Micropor. Mesopor. Mat. 109 (2008) 184–192.

[5] H. Zheng, L. Han, H. Ma, Y. Zheng, H. Zhang, D. Liu, S. Liang, Adsorption characteristics of ammonium ion by zeolite 13X Journal, J. Hazard. Mater. 158 (2008) 577–584.

[6] D. Nibou, H. Mekatel, S. Amokrane, M. Barkat, M. Trari, Adsorption of Zn^{2+} ions onto NaA and NaX zeolites: Kinetic, equilibrium and thermodynamic studies, J. Hazard. Mater. 173 (2010) 637–646.

[7] D. Nibou et al., Removal of UO_2^{2+} onto synthetic NaA zeolite: Characterization, equilibrium and kinetic studies, Chem. Eng. J. 72 (2011) 296–305.

[8] M. Zhang, H. Zhang, D. Xu, L. Han, D. Niu, L. Zhang, W. Wu, B. Tian, Ammonium removal from aqueous solution by zeolites synthesized from low-calcium and high-calcium fly ashes, Desalination 277 (2011) 46–53.

[9] G. Moussavi, S. Talebi, M. Farrokhi, R. Mojtabaee Sabouti, The investigation of mechanism, kinetic and isotherm of ammonia and humic adsorption onto natural zeolite, Chem. Eng. J. 171 (2011) 1159–1169.

[10] APHA, AWWA, WEF, Standard Methods for Examination of Water and Wastewater, American Water Work Association, Washington, DC, 1998.

[11] S. Si, A. Kotal, T.K. Mandal, S. Giri, H. Nakamura, T. Kohara, Size-controlled synthesis of magnetite nanoparticles in the presence of polyelectrolytes, Chem. Mater. 16 (2004) 3489–3496.

[12] A.M. Yusof, L.K. Keat, Z. Ibrahim, Z.A. Majid, N.A. Nizam, Kinetic and equilibrium studies of the removal of ammonium ions from aqueous solution by rice husk ash-synthesized zeolite Y and powdered and granulated forms of mordenite, J. Hazard. Mater. 174 (2010) 380–385.

[13] V. Vimonses, S. Lei, B. Jin, C.W.K. Chow, C. Saint, Adsorption of congo red by three Australian kaolins, Appl. Clay Sci. 43 (2009) 465.

[14] Z. Aksu, G. Dönmez, A comparative study on the biosorption characteristics of some yeasts for Remazol Blue reactive dye, Chemosphere 50 (2003) 1075–1083.

[15] G. Moussavi, R. Khosravi, Removal of cyanide from wastewater by adsorption onto pistachio hull wastes: Parametric experiments, kinetics and equilibrium analysis, J. Hazard. Mater. 183 (2010) 724–730.

[16] M.A. Al-Ghouti, M.A.M. Khraisheh, M.N.M. Ahmad, S. Allen, Adsorption behaviour of methylene blue onto Jordanian diatomite: a kinetic study, J. Hazard. Mater. 165 (2009) 589–598.

[17] A. Späth, B. König, Molecular recognition of organic ammonium ions in solution using synthetic receptors, Beilstein J. Org. Chem. 6 (2010) 32.

[18] L. Abramian, H. El-Rassy, Adsorption kinetics and thermodynamics of azo-dye Orange II onto highly porous titania aerogel, Chem. Eng. J. 150 (2009) 403–410.

[19] R.D. Letterman, Water Quality and Treatment, fifth ed., McGraw-Hill, Inc, Washington, DC, 1999.

[20] W.J. Weber, Jr., J.C. Morris, Kinetics of adsorption on carbon from solution, J. Sanitary Eng. Div. Am. Soc, Civ. Eng. 89 (1963) 31–60.

[21] V.J.P. Poots, G. McKay, J.J. Healy, The removal of acid dye from effluent using natural adsorbents: I peat, Water Res. 10 (1976) 1061–1066.

[22] B.H. Hameed, Evaluation of papaya seeds as a novel non-conventional low-cost adsorbent for removal of methylene blue, J. Hazard. Mater. 162 (2009) 939–944.

[23] B.H. Hameed, Spent tea leaves: a new non-conventional and low-cost adsorbent for removal of basic dye from aqueous solutions, J. Hazard. Mater. 161 (2009) 753–759.

[24] W.H. Cheung, Y.S. Szeto, G. McKay, Intraparticle diffusion processes during acid dye adsorption onto chitosan, Bioresour. Technol. 98 (2007) 2897–2904.

[25] K. Ada, A. Ergene, S. Tan, E. Yalçın, Adsorption of Remazol Brilliant Blue R using ZnO fine powder: Equilibrium, kinetic and thermodynamic modeling studies, J. Hazard. Mater. 165 (2009) 637–644.